

# Construction of a Side-Band-Separating Heterodyne Mixer for Band 9 of ALMA

F. P. Mena, J. W. Kooi, A. M. Baryshev, C. F. J. Lodewijk, R. Hesper, W. Wild, and T. M. Klapwijk.

**Abstract**—In this article we present the design, modeling and construction of a side-band-separating (2SB) heterodyne receiver for the frequency range from 600 to 720 GHz that corresponds to band 9 band of ALMA. The characteristics of this receiver present a significant improvement over the current double-side-band (DSB) configuration currently under development. The core of the mixer consists of a quadrature hybrid, two LO injectors, two superconductor-insulator-superconductor (SIS) junctions, three signal-termination loads, and two IF filtering systems. All these parts were modeled and optimized prior construction. Our 2 mixer exploits waveguide technology and has been constructed in the split-block technique. We used state-of-the-art CNC micromachining which permitted us to obtain the small dimensions required for this frequency range. The constructed receiver presents a good performance but we suggest various ideas for further improvement.

**Index Terms**— Astronomy, submillimeter wave mixers, superconductor-insulator-superconductor devices.

## I. INTRODUCTION

THE Atacama Large Millimeter Array (ALMA) is the largest radio astronomical enterprise ever proposed. Currently, it is under construction and it is expected to be operational by 2012 [1] Each of its constituting antennas will be able to hold 10 heterodyne receivers covering the spectroscopical windows allowed by the atmospheric transmission at the construction site, the altiplanos of the northern Chilean Andes. In contrast to the side-band-separating (2SB) receivers being developed at low frequencies, double-side-band (DSB) receivers are being developed for the highest two spectroscopical windows (bands 9 and 10). Despite of the well known advantages of 2SB receivers, they have not been implemented at the highest-frequency bands as the involved dimensions for some of the

This work was supported in part by NOVA, the Netherlands Research School for Astronomy, and the FP6 Radionet AMSTAR program of the European Union.

F. P. Mena, A. M. Baryshev, R. Hesper, and W. Wild are with the Netherlands Institute for Space Research and the Kapteyn Institute of the University of Groningen, Landleven 12, 9747AD Groningen, The Netherlands.

J. Kooi is with the California Institute of Technology, MS 320-47 Pasadena, California 91125, USA

C. F. J. Lodewijk and T. M. Klapwijk are with the Kavli Institute of Nanoscience, Delft University of Technology, Lorentzweg 1, 2628 CJ Delft, The Netherlands.

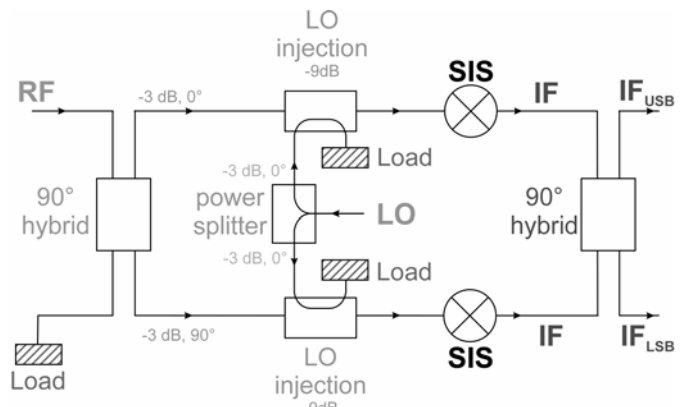


Fig. 1. Scheme of the chosen configuration for our 2SB mixer.

RF components are prohibitory small. However, the current state-of-the-art micromachining technology has proved that the complicated structures necessary for this development are attainable [2]. Here we report the design, modeling, realization, and characterization of a 2SB mixer for band 9 of ALMA. The performance is excellent and satisfies the ALMA specifications. However, further improvement can be achieved.

## II. DESIGN AND MODELING

From a variety of possible 2SB schemes, we have selected the configuration shown in Fig. 1. A  $90^\circ$  hybrid has been selected over its  $180^\circ$  counterpart despite of the superior fundamental and intermodulation product suppression capabilities of the latter. This is justified as the intrinsic parasitic capacitance of SIS junctions naturally suppresses intermodulation products and higher harmonics. Moreover, a  $90^\circ$  hybrid is simpler and, thus, easier to implement at these high frequencies [3].

We have opted for waveguide technology for the construction of the RF components and planar stripline for the IF filtering and matching parts. The current design follows previous work proposed for the balanced and correlation receivers at CSO [3]. Each one the RF components and the planar IF system (Figures 2 and 3) were modeled independently using commercial microwave-analysis software [4]. The dimensions of every RF component were selected for an optimal performance in the 600–720 GHz range. On the other hand, the IF signal is intended to cover 4–8 GHz.

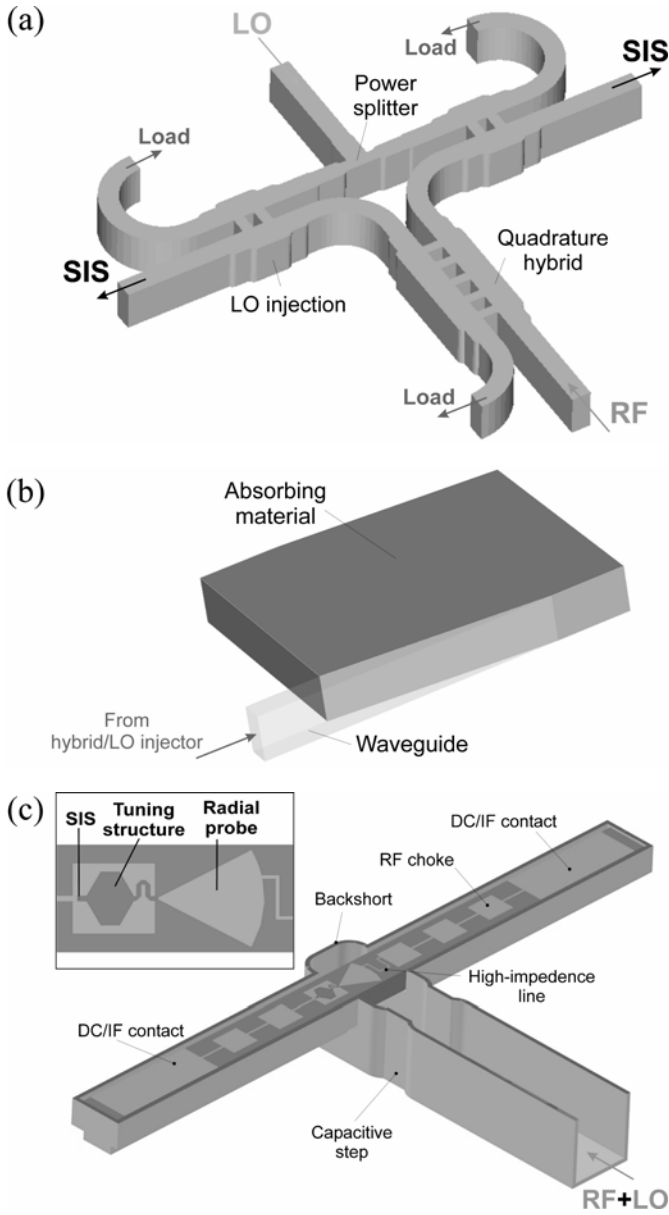


Fig. 2. Design of the various RF components: (a) Core of the 2SB mixer. (b) Signal termination load. (c) Waveguide to microstrip transition. The transversal dimensions of the waveguide are  $145 \times 310 \text{ mm}^2$ .

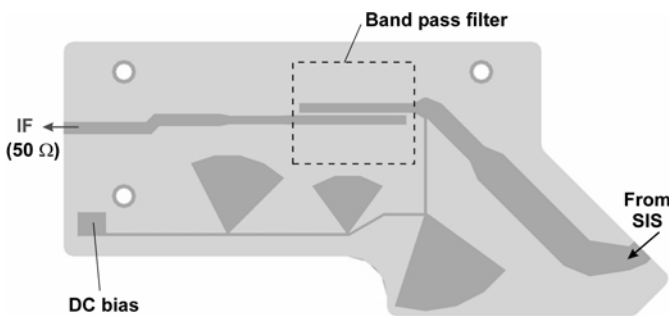


Fig. 3. IF configuration. The dashed line shows the positioning of a cutout below the substrate needed for the 3-9 GHz band pass filter.

A. RF components

In Fig. 3 we show the proposed concepts for the different RF components. The design of the power divider, LO

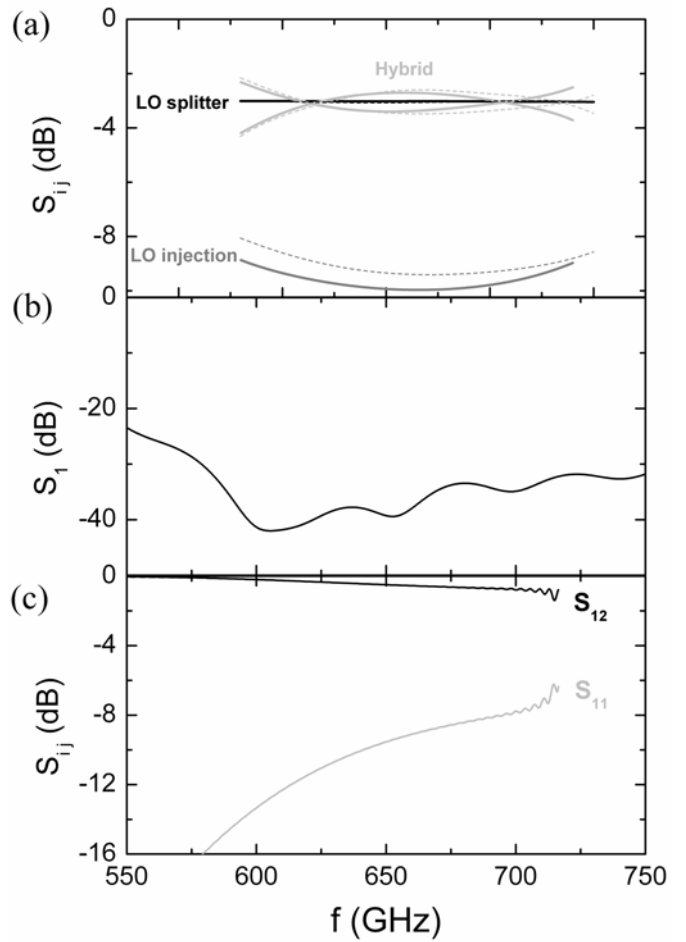


Fig. 4. Results of the electromagnetic modeling of the different RF components: (a) S-parameters between the input and output of the  $90^\circ$  hybrid, LO splitter, and LO injector as designed, solid lines, and as constructed, dashed lines. (b) Reflection coefficient of the signal termination load. (c) Coupling efficiency and return loss of the waveguide-microstrip transition.

injectors, and quadrature hybrid are based on a narrow bandwidth split block version developed for the ALMA project at lower frequencies [5]. However, at variance with that previous work, the waveguide width (b-dimension) of the present hybrid and the LO injectors has been increased by a 32.5% to maximize the thickness of the branch lines (Fig. 2) [3]. Every one of these components was simulated and optimized using commercial software. The results, summarized in Fig. 4a, show a rather flat response of the devices in our frequency window.

Although several configurations have been proposed for the signal termination loads [5]–[6], we have selected a rather novel and simple configuration which is appropriate for the small dimensions involved in the present work. The design, presented in Fig. 2(b), consists of a cavity at the end of the waveguide partially filled with an absorbing material. The geometry we are presenting here is relatively easy to make as the largest dimension is designed parallel to the splitting plane of the block. Extensive simulations of this configuration have been presented elsewhere [7]. The loads show a good performance, as demonstrated by the reflection coefficient [Fig. 4(b)], if Eccosorb MF112 [8] is used as absorbing

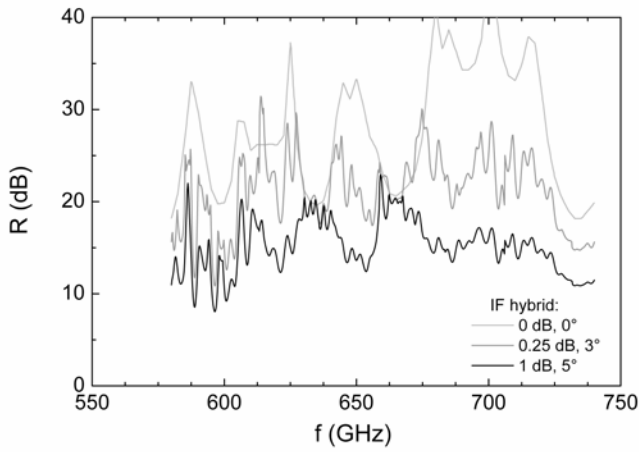


Fig. 5. Calculated sideband ratio assuming a perfect IF hybrid (light gray line) and with a amplitude and phase imbalances of 0.25 dB and 3° (gray line), and 1 dB and 5° (black line).

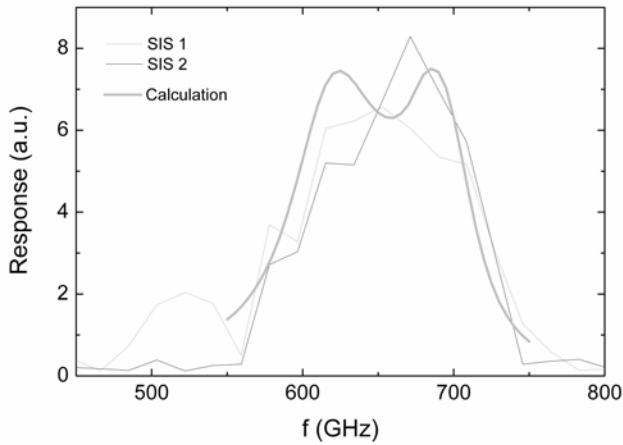


Fig. 6. Calculated and measured response of the fabricated SIS junctions. The response was measured through the RF port.

material. When the cavity is terminated at the point where the wedged part ends, large resonances appear. They can be easily damped by adding extra absorbing material. Moreover, it has also been shown [7] that this approach is pretty robust as various possible mounting errors have little influence in the overall performance.

We use a full height waveguide-to-microstrip transition to couple the incoming signal to the thin-film tuning structure of the SIS junction. The proposed structure is shown in Fig. 2(c). We have opted for a configuration that crosses the waveguide but in this case care must be taken in the way the DC bias return line meanders across the waveguide as this structure is prone to setup modal resonances. Therefore, we selected a design similar to the one proposed by Risacher et al. [9]. An important modification is that we have added a capacitive step in front of the radial probe as it improves the overall performance [10]. For the RF choke we selected the popular "rectangular" structure. The calculated coupling efficiency and return loss, between the waveguide and the tip of the radial probe, are presented in Fig. 4(c).

Given the calculated S-matrices of the different RF components, we used an S-matrix circuit simulator to calculate the sideband ratio of the complete RF core. The

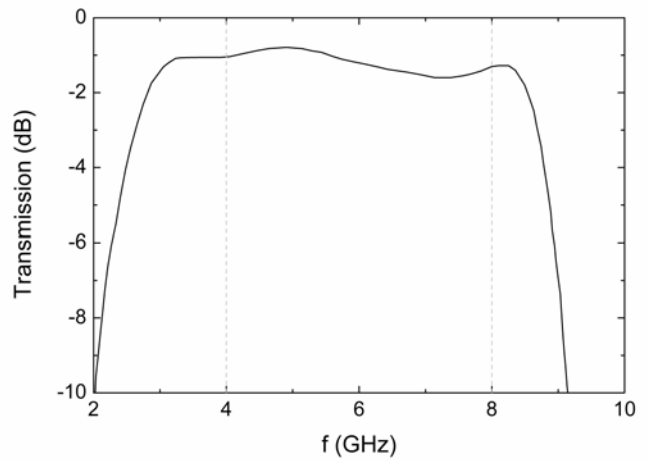


Fig. 7. Calculated transmission between the input and output ports of the IF structure presented in Fig. 3.

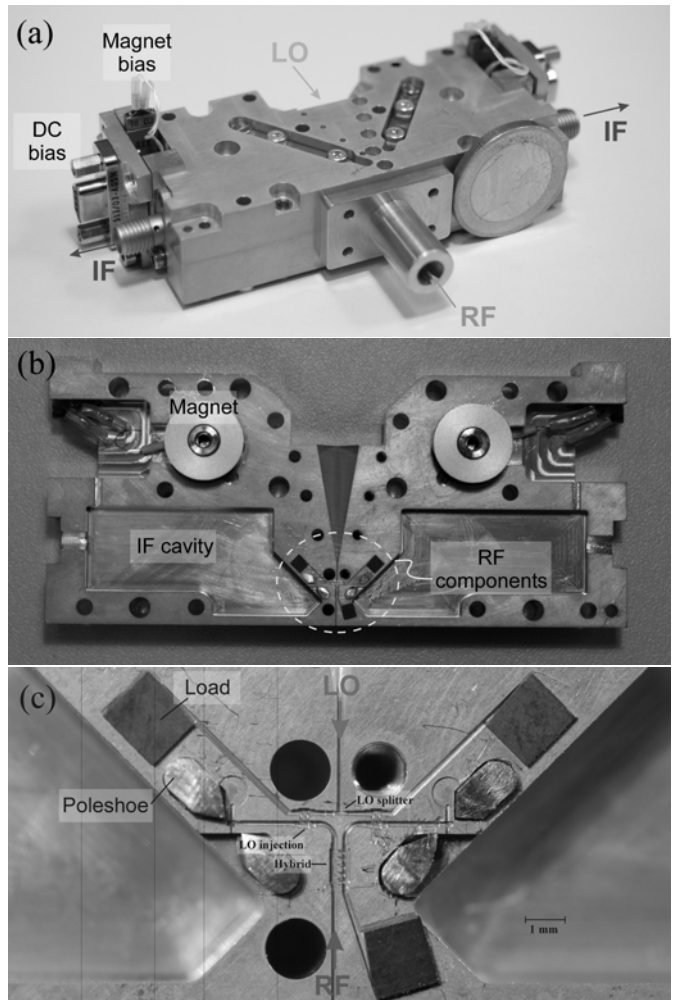


Fig. 8. Constructed 2SB block and its different components: (a) Closed 2SB block. (b) Upper half. (c) Close-up of the RF components.

results are given in Fig. 5. If a perfect IF hybrid is assumed, which will set the upper limit, a sideband ratio above 20 dB is expected across the whole band. However, the characteristics of the IF hybrid are far from ideal. We, therefore, have repeated the calculations assuming some amplitude and phase imbalance which will lower the 2SB performance.

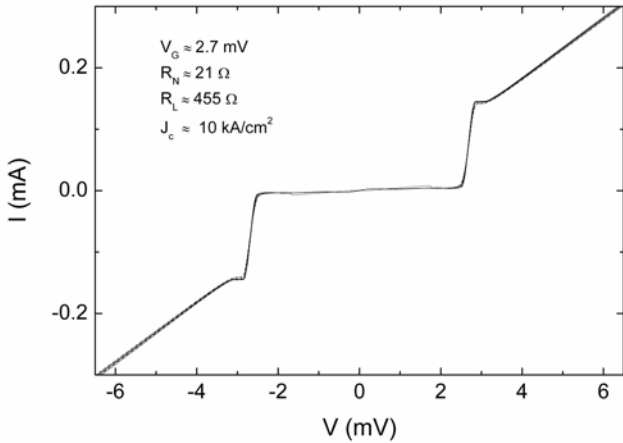


Fig. 9. IV curves of 8 different junctions. The average values of gap voltage ( $V_G$ ), normal resistance ( $R_N$ ), leakage resistance ( $R_L$ ), and critical current density ( $J_c$ ) are shown.

### B. SIS junction and tuning structure

Based in our successful experience with the development of DSB receivers for band 9 of ALMA, we have opted for a single Nb/ $\text{AlO}_x$ /Nb junction devices as detection elements for our receiver (for fabrication details, see Section III-B). Although junctions using AlN as barrier have intrinsic better properties [11], we have selected the former as, at the moment, its fabrication process is much more reliable. The reasons for which the single junction approach is preferred are twofold. First, it permits an easier suppression of the Josephson currents across the junction and, second, it allows less effort in finding reasonably matched mixers.

Given the resistance-area product,  $R_n A$ , of  $\text{AlO}_x$  junctions ( $\sim 20 \Omega \cdot \mu\text{m}^2$ ), we have selected the area of the SIS junction to be  $1 \mu\text{m}^2$  [12]. The resulting SIS impedance has to be matched with the impedance at the radial probe tip which is calculated through the electromagnetic simulation described in the previous Section. The matching is obtained by a multi-section stripline made of Nb as shown in the inset of Fig. 2(c). For a given stripline geometry, it is possible to calculate the total transmission from the radial probe tip and the SIS junction using the microscopic theory of superconductivity in the dirty limit and standard transmission line theory [13]. The geometrical parameters were changed as to get a good coverage of band 9. The result of the calculation is shown in the thick solid line of Fig. 6.

### C. Planar IF filtering and matching

To facilitate reliability and modeling, we have opted for a planar IF filtering and matching design (Fig. 3). This is a compact unit containing the IF match, DC-break, bias tee, and EMI filter. The advantage of such planar structure has been demonstrated and used in various astronomical instruments [3]. It has to be noted that, for this filter to work, the ground plane directly underneath the filter has to be removed. Previous to fabrication, the dimensions were optimized for a good performance in the 4 to 8 GHz frequency range. In Fig. 7, we show the calculated performance of the IF circuit. As shown in there, the transmission is expected to be greater than

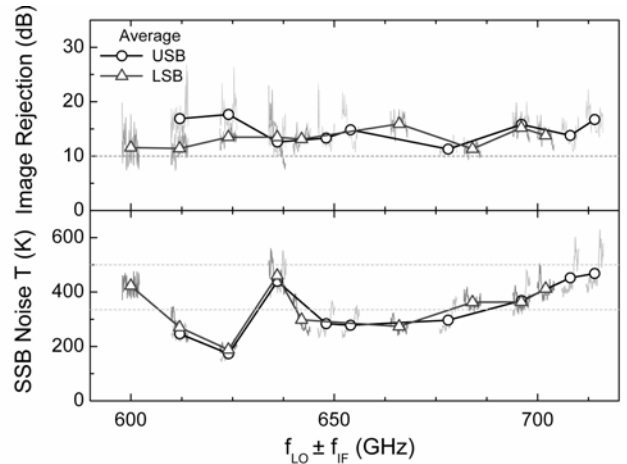


Fig. 10. Single sideband noise temperatures (bottom panel) and image rejection ratios (upper panel) at different LO frequencies. Dashed horizontal lines represent ALMA specifications for these two parameters.

$-2\text{dB}$  in the range of interest and the complex impedance limited to a small region.

## III. CONSTRUCTION

### A. Waveguide block

We have constructed the mixer in a split-block as demonstrated in Fig. 8. We have used conventional machining for the large features and CNC micromachining for the small RF features [2]. Both parts of the block were made of copper which is gold plated afterwards with a thickness of  $\sim 2 \mu\text{m}$ . The fabricated unit is rather compact ( $8 \times 2 \times 3 \text{ cm}^3$ ). It contains all the RF components, the IF filtering board, the DC biasing circuit, and the magnetic probes needed to suppress the Josephson currents in the SIS junctions. A closer inspection of the fabricated block shows that all the waveguides and cavities are approximately  $5 \mu\text{m}$  wider than designed. The reason appears to be the gold plating process as it etches away the copper that makes the block. However, the erosion is rather uniform through the entire block. To determine what the influence of this situation will be, we have repeated the simulation process with the measured dimensions (dashed lines in Fig. 4a). It is clear that our design is pretty robust as long as the symmetry is maintained.

### B. SIS junctions

The SIS devices were fabricated on a quartz substrate. First, a Nb monitor layer is deposited, after which an optically defined ground plane pattern of Nb/Al/ $\text{AlO}_x$ /Nb is lifted off. Junctions are defined by e-beam lithography in a negative e-beam resist layer and etched out with a SF<sub>6</sub>/O<sub>2</sub> reactive ion etch (RIE) using  $\text{AlO}_x$  as a stopping layer. The junction resist pattern is subsequently used as a lift off mask for a dielectric layer of SiO<sub>2</sub>. A Nb/Au top layer is deposited and Au is etched with a wet etch in a KI/I<sub>2</sub> solution using an optically defined mask. Finally, using an e-beam defined top wire mask pattern, the layer of Nb is etched with a SF<sub>6</sub>/O<sub>2</sub> RIE, finishing the fabrication process. This process renders a high yield and good reproducibility as demonstrated by the IV plots of 8

junctions (out of a sector containing 20 junctions) shown in Fig. 9.

#### IV. MIXER CHARACTERIZATION

##### A. Band coverage

The direct response, as function of frequency, of both SIS junctions contained in our mixer has been measured using a home-made Fourier transform spectrometer. The results are presented in Fig. 6. Both junctions present good band coverage and are in good agreement with the predicted response. The good agreement is obtained despite the fabrication errors discussed in the previous Section since those errors do not modify dramatically the impedances at the probe tip [Fig. 4(a)].

##### B. Noise temperature and sideband ratio

Noise temperatures ( $T_{rx}$ ) were measured using the conventional Y-factor method. As described in [14], the same setup was slightly modified to determine the sideband ratios (R)  $T_{rx}$  and R for both output bands were determined at several LO pumping frequencies and recorded as function of IF frequency. The results are summarized in Fig. 10. Both quantities are rather close to ALMA specifications as indicated by the horizontal dashed lines of Fig. 10. For  $T_{rx}$ , 80% of the band should not exceed 335 K while all points should below 500 K [15]. The image rejection ratio, on the other hand, should always be above 10 dB.

Although the noise temperature complies with ALMA specifications, it is obvious from Fig. 10 that the IF response presents a rather steep increase at high IF frequencies. The most probable reason is a mismatch between the SIS impedance and the IF unit. Further work has to be done in this aspect to improve the noise temperatures.

The obtained image rejection ratios are in close agreement with the modeling prediction given in Fig. 5 if an amplitude and phase mismatches of 1 dB and  $5^\circ$  in the IF hybrid are considered. These, indeed, are the experimental values obtained at 77 K [16]. It has to be noted that the hybrid used is a commercial one that has been optimized for operation at ambient temperature [17]. It is reasonable to argue that mismatches of 0.25dB and  $3^\circ$  can be obtained by optimization of the design at low temperatures. In that case, an improvement of  $\sim 7$  dB is expected (Fig. 5).

#### V. CONCLUSIONS

In this article we have presented the design, modeling, and realization of a side-band-separating mixer that covers the frequency range of ALMA band 9. A full test of the mixer was also presented demonstrating that complies with ALMA specifications. However, further improvement can be achieved if the IF system is optimized and AlN-barrier SIS junction technology is used.

#### REFERENCES

- [1] ALMA web site, <http://www.alma.nrao.edu/>.
- [2] Radiometer Physics GmbH, <http://www.radiometer-physics.de/>.
- [3] J. Kooi et al., "Heterodyne Instrumentation Upgrade at the Caltech Submillimeter Observatory", SPIE, Millimeter and submillimeter detectors for Astronomy II, vol. 332, pp. 5498, 2004.
- [4] Microwave Studio, <http://www.sonnetusa.com/>.
- [5] S.M.X Claude et al., "Design of a Sideband-Separating Balanced SIS Mixer Based on Waveguide Hybrids", Alma Memo 316, 2000.
- [6] A. R. Kerr et al., "MF-112 and MF-116: Compact Waveguide Loads and FTS Measurements at Room Temperature and 5 K", Alma Memo 494, 2004.
- [7] F. P. Mena and A. Baryshev, "Design and Simulation of a Waveguide Load for ALMA-band 9", Alma Memo 513, 2005.
- [8] G. A. Ediss et al., "FTS Measurements of Eccosorb MF112 at Room Temperature and 5 K from 300 GHz to 2.4 GHz", Alma Memo 273, 1999.
- [9] C. Risacher et al., "Waveguide-to-Microstrip Transition with Integrated Bias-T", IEEE Micro. and Wire. Comp. Lett., vol. 13, pp. 262, 2003.
- [10] J. Kooi et al., "A Full-Height Waveguide To Thin-Film Microstrip Transition With Exceptional Rf Bandwidth And Coupling Efficiency", Int. J. Ir. & Mm. Waves, vol. 24, pp. 261, 2003.
- [11] J. Kawamura et al., "Very high-current-density Nb/AlN/Nb tunnel junctions for low-noise submillimeter mixers". Appl. J. Phys. 76, pp. 2119, 1996.
- [12] A. R. Kerr and S.-K. Pan, "Some Recent Developments In The Design Of Sis Mixers", Int. J. Ir. & Mm. Waves, vol. 11, pp. 1169, 1990.
- [13] C. F. J. Lodewijk et al., "Improved design for low noise Nb SIS devices for Band 9 of ALMA (600 - 720 GHz)", Conf. Proc. 16th ISSTT, pp. 42, 2005.
- [14] A. R. Kerr, S.-K. Pan, and J. E. Effland, "Sideband Calibration of Millimeter-Wave Receivers", ALMA Memo 357, 2001.
- [15] W. Wild and J. Payne, "Specifications for the ALMA Front End Assembly," <http://www.cv.nrao.edu/~awooten/mmamcal/>.
- [16] S. Mahieu, Institut de RadioAstronomie Millimétrique, France, private communication, Jan. 2006.
- [17] Advanced Technical Materials Inc., <http://www.atmmicrowave.com/>.